Shielding and localization in the presence of long-range hopping

G. L. Celardo,[1,2,3,4] R. Kaiser,[5] and F. Borgonovi[1,2]

[1]*Dipartimento di Matematica e Fisica and Interdisciplinary Laboratories for Advanced Materials Physics,*
Università Cattolica, via Musei 41, 25121 Brescia, Italy
[2]*Istituto Nazionale di Fisica Nucleare, Sezione di Pavia, via Bassi 6, I-27100, Pavia, Italy*
[3]*Center for Theoretical Physics of Complex Systems, Institute for Basic Science, Daejeon, Korea*
[4]*Instituto de Física, Benemérita Universidad Autónoma de Puebla, Apartado Postal J-48, Puebla 72570, Mexico*
[5]*Université Côte d'Azur, CNRS, INLN, France*

We investigate a paradigmatic model for quantum transport with both nearest-neighbor and infinite-range hopping coupling (independent of the position). Due to long-range homogeneous hopping, a gap between the ground state and the excited states can be induced, which is mathematically equivalent to the superconducting gap. In the gapped regime, the dynamics within the excited-state subspace is shielded from long-range hopping, namely it occurs as if long-range hopping would be absent. This is a cooperative phenomenon since shielding is effective over a time scale that diverges with the system size. We named this effect cooperative shielding. We also discuss the consequences of our findings on Anderson localization. Long-range hopping is usually thought to destroy localization due to the fact that it induces an infinite number of resonances. Contrary to this common lore we show that the excited states display strong localized features when shielding is effective even in the regime of strong long-range coupling. A brief discussion on the extension of our results to generic power-law decaying long-range hopping is also given. Our preliminary results confirm that the effects found for the infinite-range case are generic.

I. INTRODUCTION

In recent years, technological advancement has allowed us to engineer several systems in which the role of quantum coherence is essential to understanding their dynamics. In view of these considerations, searching for novel coherent effects is fundamental to exploit quantum properties in technological devices such as quantum wires, quantum computers, and quantum sensors. Of particular interest is the topic of transport of energy or charge in the quantum coherent regime, due to its relevance in many technological applications, such as in light-harvesting systems [1], molecular wires [2], and in other mesoscopic systems [3].

Recently, great attention has been devoted to quantum transport in models with long-range interactions due to their relevance in many condensed matter physical systems. Indeed long-range interactions between the constituents of a system do not arise only from microscopic interactions, but in many condensed matter systems they can be induced by the coupling with environmental modes having a wavelength larger than the system size. This mediated long-range interaction arises in several systems: in ion traps [4] due to the coupling of the trapped ions with large wavelength phonon modes, in cold atoms [5], and in natural light harvesting systems [1], due to the coupling with the electromagnetic field (EMF) when the wavelength of the photon is much larger than the system size. Long-range interacting systems display particular features that are not often observed in other systems, such as broken ergodicity [6] and long-lasting out-of-equilibrium regimes [7]. Out-of-equilibrium dynamics of such models have been widely analyzed both experimentally [4] and theoretically [8–10], showing nontrivial cooperative effects and strong dependence of the dynamical evolution on the initial state. Together with a very fast spreading of information [4] and the destruction of localization [11], also the opposite behavior has been reported

in case of long-range interacting system: the suppression of information spreading [8,9,12] and strong signatures of localization [13–15].

In a recent publication [10] by some of the authors of the present paper, a common feature of long-range interacting systems was found, named cooperative shielding. This effect has been discussed in a many-body spin system in Ref. [10], where it was shown that shielding is able explain many contradictory dynamical and transport features in systems with long-range interactions, as the ones mentioned above. Indeed, contrary to the common lore, which claims that propagation of perturbation is very fast in long-range interacting systems, it was found that even in the regime of very large long-range interaction strength there are subspaces where the evolution is determined by an emergent short-ranged Hamiltonian.

Here we analyze the cooperative shielding effect in a different model: a single excitation model of transport with long-range hopping. We also discuss the consequences of such effect on transport and localization. Specifically, here we focus on models with an infinite interaction range, which are representative of the whole class of long-range interacting systems [16–18]. Despite its apparent simplicity, infinite-range hopping can be realized experimentally in ion traps [4] where linear spin chains have been recently emulated with a spin-spin interaction decaying with the distance as $1/r^\alpha$ with $0 \leqslant \alpha \leqslant 3$. The case $\alpha = 0$ corresponds to an infinite interaction range, which is discussed here. Moreover, it is routinely used to model superconductivity in ultrasmall metallic grains [19] and nonequilibrium phenomena around a phase transition in strongly correlated materials [20].

II. MODEL AND ENERGY GAP

We discuss the shielding effect by means of a paradigmatic model for quantum transport, e.g., a one-dimensional (1D)
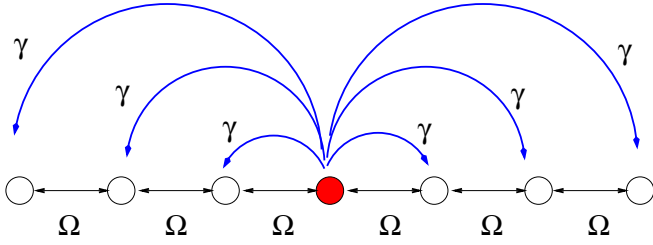
FIG. 1. Schematic representation of the model described by the Hamiltonian (1). The particle can hop through a one-dimensional ring with disordered site energies, in presence of nearest-neighbor tunneling amplitudes, Ω. V_{LR} represents the long-range (distant independent) hopping with strength γ.

Anderson model [21] (described by H_0) with N sites, with the addition of long-range hopping terms V_{LR}, having a distance-independent coupling amplitude. The Hamiltonian, see also Fig. 1, is given by:

$$H = H_0 + V_{LR} = H_{NN} + D + V_{LR}$$
$$= -\Omega \sum_i (|i\rangle\langle i+1| + \text{H.c.})$$
$$+ \sum_i E_i^0 |i\rangle\langle i| - \gamma \sum_{i \neq j} |i\rangle\langle j|. \quad (1)$$

The basis states $|j\rangle$ can represent the state of a particle localized at the site j as it is usually assumed in tight-binding models of electronic transport or, as in models of excitonic transport, an excited two-level system at site j, when all the other two-level systems are in their ground state. In Eq. (1), H_{NN} represents the nearest-neighbor hopping with $\Omega > 0$ and D the disordered part, since we assume E_i^0 to be random variables uniformly distributed in the interval $[-W/2, +W/2]$ (W is the disorder strength). In this way $H_0 = H_{NN} + D$ is exactly the Anderson Hamiltonian [21] while the long-range hopping with $\gamma > 0$ is fully contained in V_{LR}. Note that our main results are largely independent of the distribution of the site energies E_i^0.

Let us mention two important models equivalent to Eq. (1). The first is the spin system:

$$H = \sum_k h_k \sigma_k^z - 2\Omega \sum \left[\sigma_x^k \sigma_x^{k+1} + \sigma_y^k \sigma_y^{k+1}\right]$$
$$- 2\gamma \sum \left[\sigma_x^l \sigma_x^m + \sigma_y^l \sigma_y^m\right]$$

in the single excitation manifold, which can be implemented in ion trap experiments [4]. The second is the discrete BCS model [19] [which is equivalent to Eq. (1) in the limit of vanishing nearest-neighbor hopping],

$$H_{BCS} = \sum_i E_i^0 |i\rangle\langle i| - \gamma \sum_{i \neq j} |i\rangle\langle j|,$$

where $|i\rangle = |E_i^0 \uparrow; E_i^0 \downarrow\rangle$ is a Cooper pair state, where one electron occupies a single particle state with energy E_i^0 and the other one is the time-reversed state.

Let us first consider the case of no disorder $W = 0$, so that $H = H_{NN} + V_{LR}$. The eigenvalues of H_{NN} in (1) can be
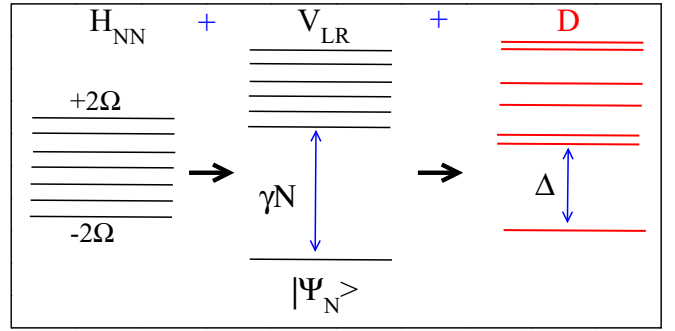

FIG. 2. Schematic representation of the energy levels of the system (1), as different terms are turned on. In the left column the spectrum of H_{NN} only is shown; middle column: creation of a gap once the long-range hopping term V_{LR} is added; right column: the effect of static disorder on the spectrum of the total Hamiltonian. Once disorder is added, the gap Δ survives only for $\gamma > \gamma_{cr}$, see Eq. (5).

computed exactly and are given by,

$$E_q^{NN} = -2\Omega \cos(2\pi q/N)$$

with $q = 1, \ldots, N$, together with the components of the eigenstates

$$\langle k | \psi_q \rangle = e^{2\pi ikq/N}/\sqrt{N} \quad (2)$$

in the site basis $|k\rangle$. The ground state, corresponding to $q = N$ and energy $E_N^{NN} = -2\Omega$,

$$|\psi_N\rangle = \frac{1}{\sqrt{N}} \sum_{k=1}^N |k\rangle. \quad (3)$$

is fully symmetric and extended in the site basis. This state is also an eigenstate of V_{LR} with eigenvalue $-(N-1)\gamma$. All the other eigenstates of V_{LR} are degenerate with eigenvalue $+\gamma$, and can always be chosen to coincide with the other eigenstates of H_{NN}, since $[H_{NN}, V_{LR}] = 0$. Note that V_{LR} has only two different eigenvalues: $-(N-1)\gamma$, which is not degenerate and $+\gamma$, which is $N-1$ degenerate. The eigenvalues of the Hamiltonian, $H_{NN} + V_{LR}$, can be written as,

$$E_q = -2\Omega \cos(2\pi q/N) + \gamma - N\gamma \delta_{qN},$$

with $q = 1, \ldots, N$. It follows that $H_{NN} + V_{LR}$ is characterized by a ground state $|\psi_N\rangle$ separated by an energy gap $N\gamma$ from the excited states, see Fig. 2 (central column).

Let us now analyze the case of $W \neq 0$. In this case $H_0 = H_{NN} + D$ does not commute anymore with V_{LR} and disorder tends to mix the two eigensubspaces of V_{LR}. To understand this point, it is convenient to write the total Hamiltonian in the eigenbasis of V_{LR}, see Eq. (2), which diagonalize $H_{NN} + V_{LR}$. In this basis D becomes a full matrix and the variance of the matrix elements $D_{qq'}$, which connect the eigenstates of V_{LR}, see Eq. (2), can be easily computed [17,18] as $\langle |D_{qq'}|^2 \rangle = \frac{W^2}{12N}$, where $\langle \ldots \rangle$ stands for the average over disorder.

Concerning the energy gap, one could expect that, for large $N\gamma$ or weak disorder strength W, the mixing between the two eigensubspaces of V_{LR} is also weak and an energy gap will be present in the spectrum of the total Hamiltonian too. Indeed, the energy gap can be computed exactly in the limit $W \gg \Omega$
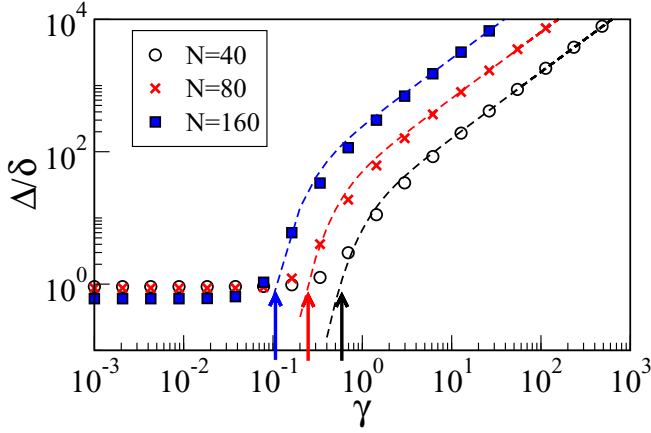
FIG. 3. Rescaled gap Δ/δ with $\delta = W/N$, average spacing between energy levels, as a function of the long-range hopping strength γ for different N values as indicated in the legend. Here $W = 100$, $\Omega = 1$. Vertical arrows indicate the critical values $\gamma_{\rm cr}$ given in Eq. (5). Dashed lines represent the Richardson solution as given in Eq. (4).

and large N and it coincides with the Richardson solution of the superconducting gap [19]:

$$\Delta = W/\sinh(W/N\gamma), \qquad (4)$$

from which we have that the gap increases with the system size, indeed $\Delta \approx 2We^{-W/N\gamma}$ for $W \gg N\gamma$ and $\Delta \approx N\gamma$ for $N\gamma \gg W$. For any finite-size system, we can talk about an energy gap only when the energy distance between the ground state and the first excited state is larger than the mean level spacing δ (average distance between the energy levels). Thus, the condition for the destruction of the gap Δ can be estimated from $\delta \simeq \Delta$. For $\gamma = 0$ and $W \gg \Omega$ one has $\delta \simeq W/N$. From the condition $\Delta/\delta \simeq 1$, we can find a critical γ, below which the gap disappears:

$$\gamma_{\rm cr} \simeq \frac{W}{N \, {\rm arsinh}(N)} \approx \frac{W}{N \ln 2N} \quad \text{for} \quad N \gg 1. \qquad (5)$$

In Fig. 3 we show the critical strength $\gamma_{\rm cr}$ as vertical arrows together with the analytical estimate given in Eq. (4). As one can see the ratio Δ/δ is well described by Eq. (4) for $\gamma > \gamma_{\rm cr}$ (compare symbols with dashed lines).

III. COOPERATIVE SHIELDING

In this section we want to analyze the cooperative shielding effect both without disorder, where it is exact, and with disorder, where it is effective for a finite time scale, diverging with the system size. As we have shown in the previous section, V_{LR} has only two eigenvalues, one corresponding to the fully symmetric state, Eq. (3), and the other one corresponding to a $N - 1$ degenerate subspace.

For $W = 0$ we have that $[H_{NN}, V_{LR}] = 0$ and the excited states of the Hamiltonian $H_{NN} + V_{LR}$ coincide with the degenerate subspace of V_{LR}. Here we show that in the excited-state subspace of $H_{NN} + V_{LR}$, the dynamics occurs as if long-range hopping would be absent and it is determined by H_{NN} only. We will show this point in two different ways.

First, let us consider a trivial and general case, i.e., a system described by $H = H_0 + V$ with $[H_0, V] = 0$. We also assume that the spectrum V is degenerate in one of its eigensubspaces $\mathcal{V}$, so that $V|v_k\rangle = v|v_k\rangle \forall |v_k\rangle \in \mathcal{V}$. The evolution of any initial state $|\psi(0)\rangle$ belonging to $\mathcal{V}$ is simply given by: $|\psi(t)\rangle = e^{-ivt/\hbar}e^{-iH_0t/\hbar}|\psi(0)\rangle$. Since the only effect of V is to induce a global phase, which has no effect on any observables, we can say that the dynamics, starting from an eigensubspace of V, is shielded from V and determined only by H_0. From the above discussion it follows that for $W = 0$, shielding in the excited-state subspace, which coincides with the eigenspace of the degenerate eigenstates of V_{LR}, is exact for any value of γ and N. In the following we will show that, even when $[H_0, V_{LR}] \neq 0$, shielding can still persist up to a very long time, diverging with the system size (cooperativity). This is rather counterintuitive, since if $[H_0, V_{LR}] \neq 0$, H_0 mixes the different eigensubspaces of V_{LR} so that one might expect a dynamics strongly dependent on V_{LR} itself.

We can show the shielding effect in the case of no disorder also considering the dynamics. For the sake of simplicity let us add a term $-\gamma \sum_i |i\rangle\langle i|$ to the Hamiltonian $H_{NN} + V_{LR}$. Such a choice corresponds to a constant energy shift equal to $-\gamma$ of the site energies and does not affect the dynamics of the system. Let us consider a generic initial state, $|\psi\rangle = \sum_k c_k|k\rangle$, written on the site basis $|k\rangle$. Evolution is given by the Schrödinger equation with Hamiltonian, $H_{NN} + V_{LR} - \gamma \sum_i |i\rangle\langle i|$, and we have:

$$i\hbar \frac{dc_k}{dt} = -\Omega(c_{k-1} + c_{k+1}) - \gamma \sum_j c_j. \qquad (6)$$

where the first term on the right-hand side represents the nearest-neighbor evolution and the second is due to long-range hopping. Equations of motion can be rewritten in terms of the macroscopic quantity :

$$Z(t) = \frac{1}{\sqrt{N}} \sum_k c_k(t),$$

namely

$$i\hbar \frac{dc_k}{dt} = -\Omega(c_{k-1} + c_{k+1}) - \gamma\sqrt{N}Z$$
$$i\hbar \frac{dZ}{dt} = (-2\Omega - \gamma N)Z, \qquad (7)$$

Note that for the ground state $|\psi_N\rangle$, see Eq. (3), we have $Z = 1$ while for all the other eigenstates $|\psi_q\rangle$ with $q = 1, \ldots, N-1$ we have $Z = 0$.

From the second equation of Eq. (7) it follows trivially that if $Z(0) = 0$ then $Z(t) = 0$ for all times. Thus, the evolution of any initial state orthogonal to the ground state (characterized by $Z = 0$), namely any combination of excited states, will be determined only by the nearest-neighbor part, as if the long-range interaction would be absent, see first equation in Eq. (7). The absence of long-range hopping in the $Z = 0$ subspace for $W = 0$ has some counterintuitive effects. For instance in the absence of the nearest-neighbor interaction, if we start with a particle in an antisymmetric superposition on two sites, so that $Z = 0$, we have that the particle will not go anywhere, despite the distance-independent tunneling hopping amplitude that connects all the sites.

Note that, for the case of no disorder, shielding from long-range interaction involves a subspace of dimension $N - 1$ (all the eigenstates orthogonal to the ground state $|\psi_N\rangle$ of $H_{NN} + V_{LR}$ satisfy the condition $Z = 0$) thus including almost the whole Hilbert space.

The question we want to address now if whether this effect survives in presence of disorder, which breaks the symmetry of the system so that the V_{LR} does not commute anymore with the rest of the Hamiltonian. Disorder also tends to mix the two eigensubspaces of V_{LR} and this could lead, in general, to the destruction of shielding in the excited states. Indeed, in presence of disorder, the excited states do not lie completely in the degenerate subspace of V_{LR}, so that a random initial state in the excited-state subspace will in general have components in more than an eigensubspace of V_{LR} and thus V_{LR} can be relevant for its dynamics. Nevertheless, even for $W \neq 0$ and in the regime of large gap $\gamma \gg \gamma_{\rm cr}$, the mixing between the two eigensubspaces of V_{LR} induced by disorder, is weak. Under these conditions any initial state in the excited subspace of H will mainly lie in the degenerate subspace of V_{LR} so that it will be dynamically shielded from the long-range term for a very long time. Interestingly, on increasing the system size, the gap, see Eq. (4), increases and shielding becomes stronger as it will be shown below.

A. A qualitative dynamical analysis

In this section we will give a qualitative analysis of the shielding effect based on the dynamics. We choose as initial state $|\psi_{\rm in}\rangle$ a random superposition of the excited states of H and we compare its time evolution (in the regime $\gamma \gg \gamma_{\rm cr}$) under both the full Hamiltonian H and the Anderson Hamiltonian H_0 (which does not contain the long-range term). In order to have a consistent spreading of the initial wave packet we chose a small value of disorder $W/\Omega = 1$. In Fig. 4 we plot the probability distribution in the site basis at a fixed time T for two different N values. While for small N the unperturbed and full dynamics give completely different results (top panel), for a sufficiently large N value the two distributions are close one to each other (bottom panel) showing how on increasing N (cooperativity) at fixed time T the full dynamics occurs as if long-range hopping would be absent (shielding). This simple example shows that the presence of a gap (the condition $\gamma > \gamma_{\rm cr}$ is verified in both panels of Fig. 4) is not enough to have shielding, which can thus be defined only within a suitable time scale. This point will be discussed in Sec. III B.

Note that in the regime of large gap shielding is effective only for an initial state, which lies in the excited-state subspace. On the other hand, for initial states with a strong component on the ground state, shielding will not be effective. Indeed in this case the initial state will have large components on eigenstates of V_{LR} with different eigenvalues, so that V_{LR} can impact the dynamics. To illustrate this point, let us consider another initial condition $|\Phi_{\rm in}\rangle = 1/\sqrt{2n+1} \sum_{k=-n}^{k=n} |k\rangle$ with $n = 4$, which has strong components on both eigensubspaces of V_{LR}. As one can see from Fig. 5, as N increases the shielding effect does not occur, contrary to the other initial conditions considered in Fig. 4 for the same parameters.
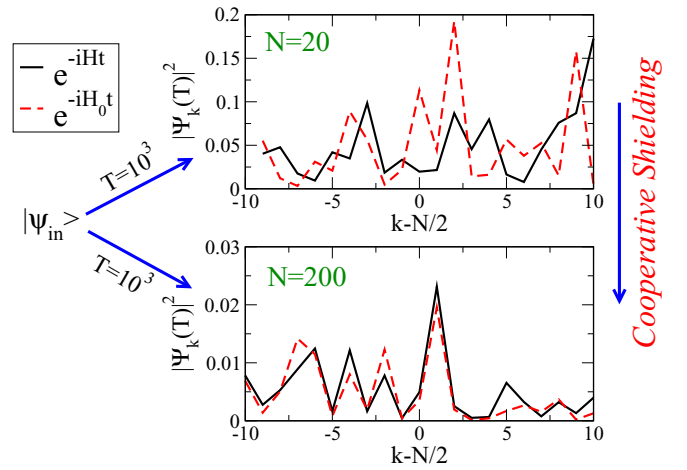

FIG. 4. Probability to be on the kth site, at the time $T = 10^3$ for $N = 20$ (top) and $N = 200$ (bottom). In both panels, full black lines have been obtained by evolving the initial state $|\psi_{\rm in}\rangle$ with the full Hamiltonian H, while the red dashed curves are obtained with H_0, see Eq. (1). The initial state $|\psi_{\rm in}\rangle$ has be chosen to be a random superposition of the excited states of H. Other data are $\Omega = 1, W = 1, \gamma = 1$ and we are in the regime $\gamma > \gamma_{\rm cr}$, see Eq. (5).

B. Time scale of fidelity decay

To analyze in a more quantitative way the shielding effect, we consider the fidelity, defined as the overlap probability between a state evolved with the full Hamiltonian (1) and that evolved with $H_0 = H_{NN} + D$ (without the long-range term). As initial condition we choose a state $|\psi_{\rm in}\rangle$ composed by a random superposition of all the excited states of H, and we compute the fidelity as:

$$F_{H_0}(t) = |\langle\psi_{\rm in}|e^{iH_0t/\hbar}e^{-iHt/\hbar}|\psi_{\rm in}\rangle|^2. \qquad (8)$$

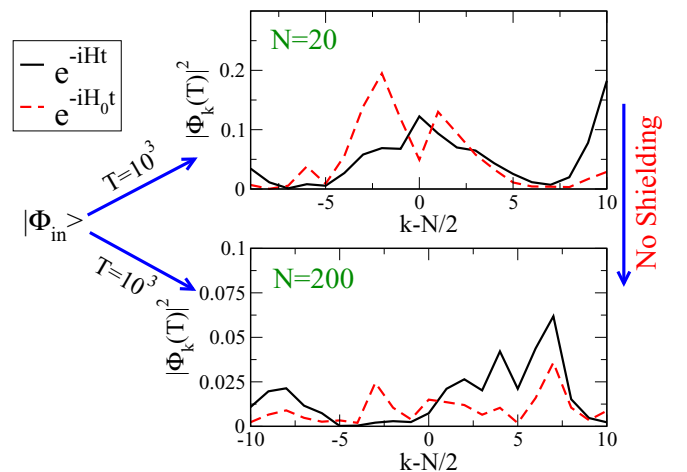Examples of fidelity decay in time are reported in Fig. 6.

FIG. 5. Probability to be on the kth site, at the time $T = 10^3$ for $N = 20$ (top) and $N = 200$ (bottom). In both panels, full black lines have been obtained by evolving the initial state $|\Phi_{\rm in}\rangle$ with the full Hamiltonian H, while the red dashed curves are obtained with H_0, see Eq. (1). The initial state $|\Phi_{\rm in}\rangle$ has be chosen to be a superposition of the excited states and the ground state of H, see text. Other data are $\Omega = 1, W = 1, \gamma = 1$ and we are in the regime $\gamma > \gamma_{\rm cr}$, see Eq. (5).
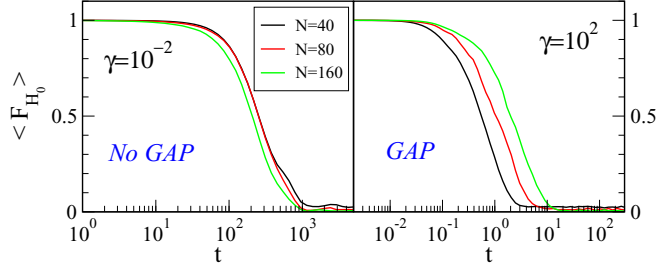
FIG. 6. Average fidelity vs time starting from a random superposition of the $N-1$ excited states and different N values as indicated in the legend. Left: small coupling $\gamma = 10^{-2} < \gamma_{cr}$; right: large coupling $\gamma = 10^2 > \gamma_{cr}$. Other data are $\Omega = 1, W = 100$.

In the two panels of Fig. 6 the behavior of the average fidelity, see Eq. (8), $\langle F_{H_0} \rangle$, taken over different random realizations vs time is shown in two different regimes (above and below γ_{cr}), see Eq. (5). As one can see, while for $\gamma \ll \gamma_{cr}$ (gapless region) the fidelity decay is almost independent of the system size, the shielding effect manifests itself for $\gamma \gg \gamma_{cr}$ (gapped region) where the fidelity increases with the system size.

If shielding would be perfect, fidelity would remain equal to one for all times. Thus, to quantify shielding we use the time $\tau_{1/2}$ at which the average (over disorder) fidelity decreases to one half. This shielding time $\tau_{1/2}$ rescaled to the system size is plotted in Fig. 7 vs γ/γ_{cr} for different system sizes. For a fixed W, all data collapse on a single curve given by

$$\frac{\tau_{1/2}}{N} = \begin{cases} c_1 \frac{\gamma_{cr}}{\gamma} & \text{for} \quad \gamma \ll \gamma_{cr}, \\ \frac{c_2}{W} & \text{for} \quad \gamma \gg \gamma_{cr}, \end{cases} \tag{9}$$

where $c_{1,2}$ are fitting constants. From Eq. (9) it follows that for $\gamma \ll \gamma_{cr}$, one has $\tau_{1/2} \propto W/[\gamma \ln(2N)]$. Since γ represents the strength of the perturbation, it is expected that fidelity decays faster as γ increases. Note also that $\tau_{1/2}$ decreases with N in this regime. On the other hand when $\gamma \gg \gamma_{cr}$
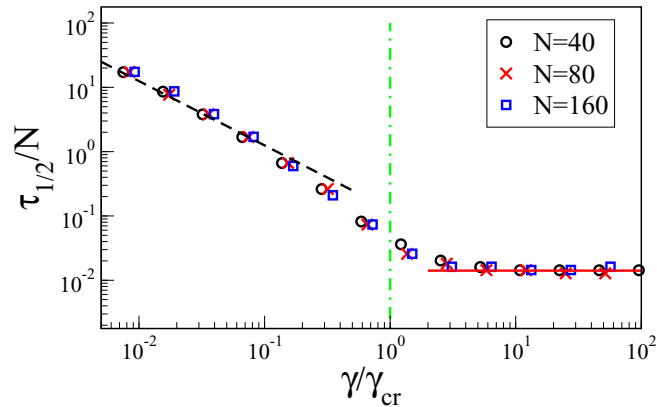

FIG. 7. Rescaled half time $\tau_{1/2}/N$ vs γ/γ_{cr} for different N values as indicated in the legend. As initial state a random superposition of the $N-1$ excited states has been chosen. Other data are $\Omega = 1, W = 100$. Horizontal full line represents the theoretical prediction, $\tau_{1/2}/N = c_2/W$ in the gapped regime. The dashed line stands for $c_1 \gamma_{cr}/\gamma$. $c_{1,2}$ are fitting constants. The vertical dot-dashed line is $\gamma = \gamma_{cr}$.

(gapped regime), we have $\tau_{1/2} \propto N/W$, which means that the shielding time becomes completely independent of the long-range coupling strength γ (shielding) and it increases with the system size (cooperativity). The expression $\tau_{1/2} \simeq N/W$ in the gapped regime can also be obtained analytically (see Appendix A). Let us stress that this behavior is peculiar to the homogeneous long-range hopping. Indeed if one considers the case of random long-range hopping, namely a random coupling between different sites, there is no gap in the spectrum of the Hamiltonian and $\tau_{1/2}$ always decreases with γ as expected (see Appendix A).

IV. CONSEQUENCES OF SHIELDING ON PROPAGATION OF PERTURBATIONS

Here we show the consequences of the shielding effect on the velocity of propagation of perturbations, which is a major topic of investigation in recent literature. In particular one of the main questions is to understand whether the propagation of excitations in systems with long-range interaction remains or is not confined to an effective light cone [4,8,9,22–27], as defined by the Lieb-Robinson bound [28] and its generalizations (see Ref. [9] and references therein). Indeed in systems with nearest-neighbor interaction, it has been proven [28] that the propagation of perturbations has a finite velocity proportional to the nearest-neighbor coupling strength and independent of the system size, so that it defines an effective light cone. Outside such light cone, the propagation is exponentially suppressed. On the other hand, in recent experiments with trapped ions, it was observed that for long-range interaction, the light-cone picture is no longer valid, the dynamics becomes nonlocal, and perturbations propagate nonlinearly in time.

This subject has been recently discussed in Ref. [10] by some of the authors of this paper. There it is shown that, due to cooperative shielding, together with very fast spreading of perturbations, a long-range interacting system can also display freezing or effective short-ranged dynamics (constrained within a light cone). This occurs if the initial conditions belong to a shielded subspace, and it is valid for a finite time, which increases with the system size.

Here we analyze the propagation of perturbations in our transport model. Specifically, we start from an excitation shared antisymmetrically between two nearest-neighbor sites: $|\psi_0\rangle = (|N/2\rangle - |N/2 - 1\rangle)/\sqrt{2}$. Note that such state belongs to the degenerate eigensubspace of V_{LR} with $Z = 0$. We let the state evolve with the full Hamiltonian and compute the probability to be at time t on site i along the chain. The results are shown in Fig. 8. In Figs. 8(a), 8(c) we change only the long-range coupling strength γ, while in Figs. 8(b), 8(d) we change only the nearest-neighbor coupling Ω, keeping all parameters fixed. As one can see, the velocity of propagation describes a linear light cone in all cases, up to the time scale given in the figure, despite the presence of long-range coupling. In particular the shielding effect has the striking consequence that the velocity of propagation is proportional to Ω, but completely unaffected by increasing γ.

In order to confirm the cooperative nature of the shielding effect, in Fig. 9 we analyze the spreading of perturbations as the system size is varied, keeping all other parameter fixed. As
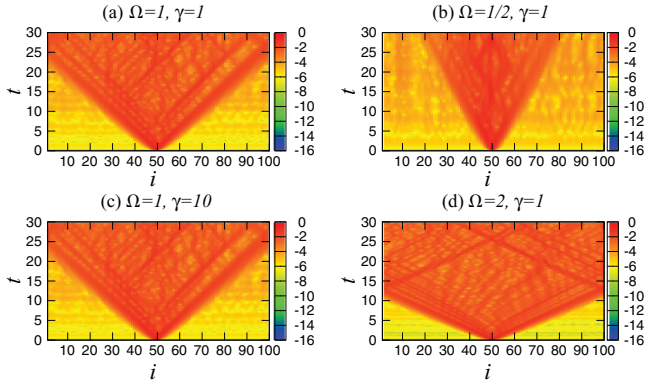
FIG. 8. Probability (in log scale) to be on site i at time t. The dynamics has been computed starting from the initial state $|\psi_0\rangle = (|N/2\rangle - |N/2 - 1\rangle)/\sqrt{2}$. Common parameters for all panels are $N = 100, W = 1$. In (a), (c) we change γ keeping all other parameters fixed, showing that the velocity of propagation of the initial perturbation is independent of γ (long-range coupling strength) within the time scale in the figure. In (b), (d) only Ω (nearest-neighbor hopping strength) is changed, keeping all other parameter fixed, showing that the velocity of propagation is proportional to Ω.

one can see, as the system size increases, the linear propagation of perturbations holds for longer times.

The results shown in this section clarify the consequence of the shielding effect on the spreading of perturbations: due to shielding, even in presence of a large long-range coupling strength, the spreading of perturbation can be linear, as in the case of a short-ranged dynamics. We have also shown that the time for which the propagation is linear increases with the system size. On the other hand, for different initial conditions, shielding is no longer effective, as it was shown in Fig. 5, and the spreading of perturbations can be very fast [4]. In this sense shielding is able to explain the contradictory behavior of long-range interacting systems.
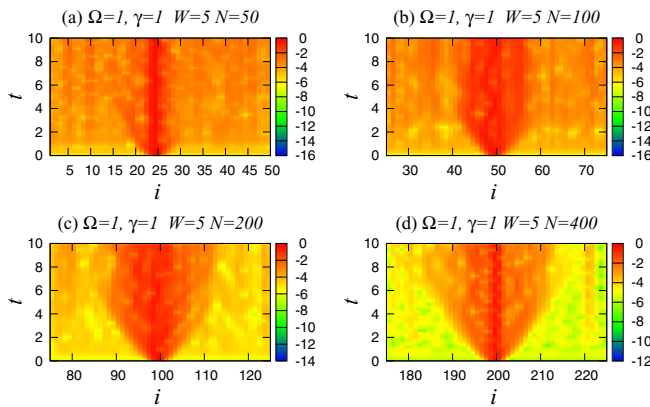

FIG. 9. Probability (in log scale) to be on site i at time t. The dynamics has been computed starting from the initial state $|\psi_0\rangle = (|N/2\rangle - |N/2 - 1\rangle)/\sqrt{2}$. Common parameters for all panels are $\Omega = 1, \gamma = 1, W = 5$. As the number of sites increases, linear propagation of perturbations holds for longer times, confirming the cooperative nature of the shielding effect.

V. CONSEQUENCES OF SHIELDING ON LOCALIZATION

In 1D tight-binding models with short-range interaction the addition of disorder induces localized eigenstates thus suppressing transport [21]. It is also commonly understood that the presence of long-range hopping terms destroys localization [11]. The following argument, for any dimension, had been usually advocated: a particle in a specific site can tunnel to a distance R under the resonant condition $V \geqslant \Delta E$, where ΔE is the energy difference between the two sites and $V = \gamma/R^\alpha$ is the tunneling coupling between them. Since the site energies are uniformly distributed between $-W/2$ and $W/2$, the probability to satisfy the resonance condition is $\approx V/W$. The number of sites enclosed in two spheres of radius R and $2R$ is proportional to R^d, where d is the embedding dimension of the lattice network, so that the number of resonant sites $N_{res} \propto V R^d / W \propto R^{d-\alpha}$. We can conclude that for short-range hopping $\alpha > d$, N_{res} goes to zero with the distance R, while for long-range hopping $\alpha < d$ it diverges with R. This general argument generates the expectation that localization can occur only for short-range hopping.

For random long-range hopping this argument agrees with the results reported in literature, see Ref. [11] and Appendix B. On the other hand for homogeneous long-range hopping, which is our case, the situation is different: even if we have an infinite number of resonances, shielding induces localization in the excited-state subspace. In order to show this point, let us consider an initial state in which only one site is occupied $|\psi_0\rangle = |1\rangle$. We consider the case in which $W/\Omega \gg 1$, so that without long range the system would be highly localized and the excitation would not spread much on the other sites in time. We also set $\gamma \gg W$ so that the initial site is almost at resonance with all the other sites. Let us compute the average over disorder survival probability $\langle P_0(t)\rangle$, where $P_0(t) = |\langle\psi_0|\psi(t)\rangle|^2$. In Fig. 10 the average survival probability is plotted vs time for different system sizes. For $N = 2$, site $|1\rangle$ is at resonance with site $|2\rangle$, so that $P_0(t)$ oscillates between the two sites. On increasing the system size, one might expect $P_0(t)$ to decrease faster with the number of sites. Indeed the long-range coupling is independent of the distance and site $|1\rangle$ is at resonance with all other sites. Contrary to this expectation, the probability to leave the initial site decreases with the number of sites. The results presented in Fig. 10 show that localization is enhanced
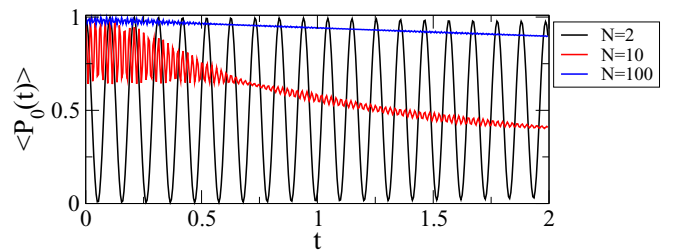

FIG. 10. Average survival probability vs time for different system sizes, see legend. At time $t = 0$ only one site is occupied. Here is $\gamma = 30 \gg W \gg \Omega$ so that the occupied site is at resonance with all the other sites. Nevertheless as the system size increases, the probability to find the system in the initial site increases.

on increasing the system size. How can we relate such results with the cooperative shielding effect? In the large N limit, the ground state of the system is well approximated by the state $|\psi_N\rangle$, Eq. (3), which represents a symmetric superposition of a particle on all sites. An initial state localized only on one site has a probability $1/N$ to be on the ground state and a probability $(N-1)/N$ to be in the excited states, so that in the large N limit a localized initial condition lies mainly in the excited-state subspace. As it has been shown in the previous sections, the excited states are shielded from long-range interaction and the dynamics in such subspace is mainly determined by H_0, so that localization becomes possible. Again, both shielding and cooperativity are shown by these results.

In order to elucidate this point in a more quantitative way, we study the participation ratio [29]

$$PR = \left\langle 1 \middle/ \sum_i |\langle i|\psi\rangle|^4 \right\rangle, \qquad (10)$$

of the eigenstates $|\psi\rangle$ of the Hamiltonian (1), where $\langle\ldots\rangle$ stands for the ensemble average over different realizations of the static disorder. For extended states, it increases proportionally to the system size, N, while, for localized states, it is independent of N.

In Fig. 11, top panel, the average PR of all the excited states is shown as a function of the rescaled long-range hopping strength γ/γ_{cr} for different system sizes. As one can see all points almost collapse in a single curve, showing that the PR depends only on γ/γ_{cr}. Moreover, above γ_{cr}, the PR reaches a constant value, which means that it also becomes independent of N. This result shows that the excited states localize above γ_{cr}, Eq. (5), for which the gap in the spectrum opens and shielding becomes effective. This is at variance with the random long-range hopping model for which localization does not occur, and the average PR never becomes independent
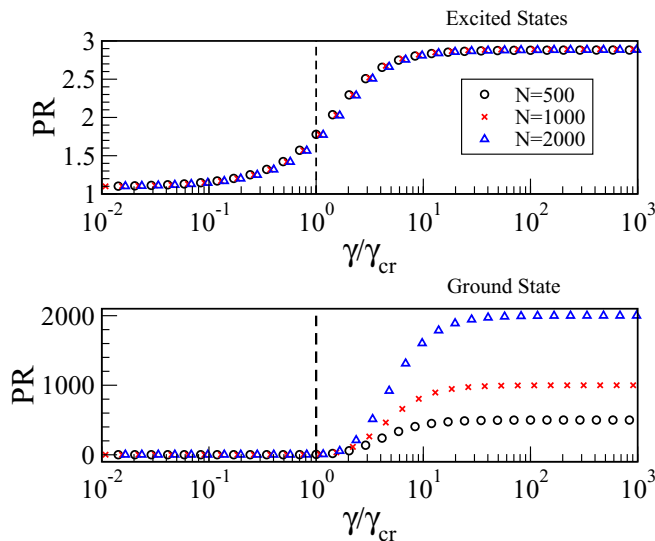

FIG. 11. Top: average participation ratio over the excited states *vs* γ/γ_{cr} and different system size. Bottom: Participation ratio for the ground state. Vertical dashed lines in both panels stand for $\gamma = \gamma_{cr}$. Other parameters are $\Omega = 1, W = 100$.

of the system size, as it is shown in Appendix B. In the gapped regime $\gamma > \gamma_{cr}$ where the PR of the excited states becomes independent of the system size, the excited states display an hybrid nature, with an exponential localized peak and a distant independent plateau, in close analogy with the results presented in Refs. [14,15].

We note that signatures of localization in presence of homogeneous long-range hopping have already been discussed in Refs. [13–15]. Here we show the deep connection with the shielding effect: since the dynamics of the excited states is shielded from long-range hopping, strong signatures of localization can arise.

Finally, let us mention that the ground state behaves differently: when $\gamma > \gamma_{cr}$, it becomes delocalized ($PR \propto N$), see Fig. 11 (bottom panel). Indeed, in this regime, a simple perturbative argument shows that the ground state is close to the state $|\psi_N\rangle$, Eq. (3), which is extended. This implies that in the gapped regime we have a coexistence of extended (ground state) and localized states (excited states) in the same region of parameters. This might be used to control transport in mesoscopic devices [30].

VI. GENERALIZATION TO POWER-LAW DECAYING LONG-RANGE HOPPING

In the previous sections we considered the case of a distance-independent long-range hopping, Here we present some preliminary results on the case of a power-law decaying long-range hopping. We will mainly analyze the localization properties of the eigenstates and from this analysis we will conjecture that shielding is a generic properties of homogeneous long-range hopping.

The model given in Eq. (1) is modified as follows:

$$\begin{aligned} H &= D + H_{NN} + V_{LR} \\ &= \sum_i E_i^0 |i\rangle\langle i| - \Omega \sum_i (|i\rangle\langle i+1| + |i+1\rangle\langle i|) \\ &\quad - \gamma \sum_{i\neq j} \frac{|i\rangle\langle j|}{|i-j|^\alpha}. \end{aligned} \qquad (11)$$

All the terms are the same as Eq. (1), except for the last term V_{LR}, which now represents a long-range hopping term, which connects all the sites of the 1D chain with an amplitude, which decays as a power law with the distance between the sites $1/r^\alpha$. α is the exponent, which determines the range of the interaction: for $\alpha = \infty$ the interaction involves only nearest-neighbor sites, while for $\alpha = 0$, the interaction does not decay with the distance and all the sites are coupled with the same strength, all-to-all interaction. For $\alpha \leqslant 1$ the hopping is long range, while for $\alpha > 1$ the hopping is short range, according to the usual definition of the range of the interaction [16]. Here, as in Eq. (1), periodic boundary conditions are assumed both for the nearest-neighbor and the long-range interaction.

Let us first analyze the case $W = 0$. The most interesting feature of the spectrum of $H_{NN} + V_{LR}$ is the presence of an energy gap, Δ_0 between the ground state and the first excited state in the case of long-range coupling. While for the case $\alpha = 0$ we have shown that $\Delta_0 = N\gamma$, from the exact solutions

of the eigenvalue problem, see Appendix C, we have for any α:

$$\Delta_0 \propto \begin{cases} \gamma N^{1-\alpha} & \text{for} \quad \alpha \leqslant 3 \\ \gamma N^{-2} & \text{for} \quad \alpha > 3 \end{cases}. \quad (12)$$

From this expression, we have that the gap increases with the system size for long-range interaction $\alpha < 1$, it is constant for the critical case $\alpha = 1$ and it decreases with the system size for short-range interaction $\alpha > 1$. Note that the existence of an energy gap between the ground state and the first excited state is a peculiar feature of the long-range nonrandom hopping interaction. Indeed for random long-range hopping there is no energy gap. Clearly the energy gap in the spectrum will survive even in presence of disorder if the disorder strength is much smaller than the energy gap.

One may wonder whether cooperative shielding is also present for generic long-range systems $\alpha < 1$. For generic long-range hopping, the gap implies that the subspace of the eigenstates of V_{LR} orthogonal to the fully symmetric state Eq. (3), will become invariant in the large N limit. On the other hand, such subspace is no longer characterized by only one eigenvalue of V_{LR} as in the case $\alpha = 0$, see analysis in Appendix C. Thus we cannot expect that H_0 will alone determine the dynamics in such subspace. We leave to a future work the detailed analysis of the shielding effect for generic long-range hopping. Instead, here we analyze the localization properties only and from this analysis we will infer that shielding is present also for generic long-range hopping.

In Fig. 12 (top) the participation ratio, see Eq. (10), averaged over disorder is shown as a function of energy for the case $\alpha = 1/3$. Only the high-energy part of the spectrum is shown. The results in Fig. 12 (top) show that high-energy states have a participation ratio independent from the system size, which is a clear sign that features of Anderson localization can be preserved even in the presence of long-range hopping. This result is consistent with the conjecture that cooperative shielding exists also in generic long-range hopping systems. Indeed, in order to have localization we need the long-range hopping to become effectively short ranged or to be strongly suppressed in a given subspace. This was the case for $\alpha = 0$ where long-range hopping is strongly suppressed and it disappears in the large N limit.

Let us now discuss the localization properties of the ground state. In the previous sections it was also shown that the ground state for the $\alpha = 0$ case shows cooperative robustness to disorder, meaning that the disorder needed to localize it increases with the system size. Our numerical simulations confirm that these features are also present for the Hermitian long-range hopping considered here for generic $\alpha < 1$. Specifically, disorder must be larger than the gap to localize the ground state and we can write for the critical disorder: $W_{cr} \approx \Delta_0 \propto N^{1-\alpha}$ for $\alpha < 1$. This is is confirmed in Fig. 11 (bottom) where the participation ratio of the ground state for the case $\alpha = 1/3$ is shown for different system sizes. We have also checked other values of $\alpha < 1$, not shown here.

Thus we have found some general properties of tight-binding models with nonrandom long-range hopping: a ground state, which shows cooperative robustness to disorder, remaining extended in the large N limit, and at the same time a part of the excited-state subspace, which shows strong signature of localization despite the presence of long-range hopping.
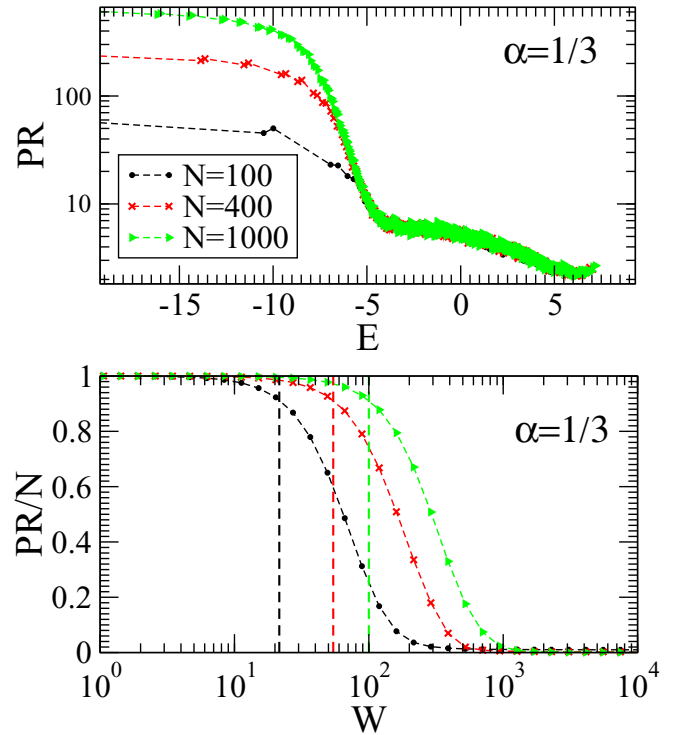

FIG. 12. Top: Participation ratio is shown vs energy for the eigenstates of the system described by Eq. (11), for different system sizes. Only the higher-energy portion of the spectrum is shown. In the bottom panel the participation ratio of the ground state divided by the number of sites is shown vs the disorder strength. As a dashed vertical line the estimated critical disorder for the onset of localization is shown. The critical disorder scales as $\gamma N^{1-\alpha}$. Parameters used in this figure are: $\Omega = \gamma = 1$, $\alpha = 1/3$ and $W = 10$.

VII. CONCLUSIONS AND PERSPECTIVES

The cooperative shielding effect has been analyzed in a paradigmatic model of single excitation quantum transport, described by a Hamiltonian $H = H_0 + V_{LR}$, where H_0 is the usual Anderson model, which contains only nearest-neighbor hopping and on-site random energies, and V_{LR} represents a distance-independent homogeneous long-range hopping. The homogeneous long-range hopping induces a gap between the ground state and the excited states of the system, which has the same mathematical nature of the superconducting gap in ultrasmall grains. In the regime of large gap, the dynamics of the excited states is described only by H_0, as if long-range would be absent (shielding), up to a time scale, which increases with the system size (cooperativity). Thus, in the excited-state subspace, H_0 constitutes an emergent Hamiltonian, valid up to a finite time scale. Such shielding effect has a strong impact on the transport properties of the system, allowing for the excited states to show strong signatures of localization, even in presence of an infinite number of resonances. Shielding from long range does not depend on the particular form of H_0 and it is determined only by the strength of the long-range hopping term V_{LR}. We believe that the results presented here for the infinite interaction range unveil common cooperative features of long-range hopping systems. Indeed our preliminary analysis of generic long-range hopping, have

shown that a strong signature of localization arises for any homogeneous long range. This result supports our conjecture that shielding is a generic property of long-range hopping. In perspective it would be interesting to determine the emergent Hamiltonian, which drives the dynamics in the localized part of the spectrum, for generic long-range hopping systems. Note that the shielding effect in single excitation transport models can be currently tested, for instance, in ion trap experiments. Moreover, the shielding effect can allow for localization to occur in relevant systems with nonrandom long-range hopping, such as in cold atomic clouds, where the issue of localization of light is one of the main open problems.

ACKNOWLEDGMENTS

We acknowledge useful discussions with R. Bachelard, G. G. Giusteri, S. Flach, M. Kastner, F. Izrailev, A. M. Martínez-Argüello, E. A. Yuzbashyan, and L. Santos.

APPENDIX A: ANALYTICAL ESTIMATE OF THE SHIELDING TIME

Here we estimate the time $\tau_{1/2}$ needed to fidelity, see Eq. (8), to decay to $1/2$. We will limit our considerations to the case $W \gg \Omega$. Following Refs. [20,21], it is possible to obtain an analytical expression for the eigenstates $|E\rangle$ of H in the regime $\gamma \gg \gamma_{cr}$. Clearly one eigenstate is very close to $|\psi_N\rangle$, see Eq. (3) (due to the presence of a large energy gap). All the other $N-1$ eigenstates can be written as:

$$|E\rangle = \frac{1}{\sqrt{C_E}} \sum_{E_0} \frac{1}{E - E^0} |E^0\rangle \qquad (A1)$$

with

$$\sum_{E_0} \frac{1}{E - E^0} = 0 \qquad (A2)$$

and where C_E is a normalization factor. In Eq. (A1), $|E_0\rangle$ and E_0 are, respectively, the eigenstates and eigenvalues of the Anderson model with Hamiltonian: $H_0 = H_{NN} + D$, see Eq. (1). From Eq. (A2) it is clear that the energies E must lie between two neighbouring energies (E_0^1, E_0^2) of H_0, so that the main contribution to the eigenstates $|E\rangle$ comes from the eigenstates of H_0 corresponding to such neighboring energies. Thus, approximating the initial state as $|E\rangle \simeq c_1 |E_0^1\rangle + c_2 |E_0^2\rangle$, we have for the fidelity,

$$F_{H_0} = \left| |c_1|^2 + |c_2|^2 e^{i(E_0^1 - E_0^2)t} \right|^2.$$

Since the mean level distance $(E_0^1 - E_0^2)$ for the eigenstates of H_0 is W/N (for $W \gg \Omega$), we can estimate the decay time for the averaged fidelity as,

$$\tau_{1/2} \propto \frac{N}{W}, \qquad (A3)$$

which is confirmed in Fig. 13.

APPENDIX B: RANDOM HOPPING MODEL

In order to show that shielding is due to homogeneous long-range hopping, here we consider the same model of Eq. (1),
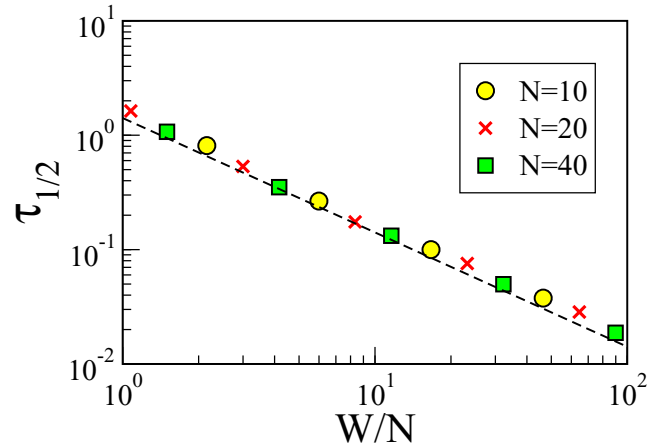

FIG. 13. Half time for the fidelity decay, $\tau_{1/2}$, vs the normalized disorder strength W/N, for different N values, as indicated in the legend. All data are in the regime $\gamma \gg \gamma_{cr}$. Symbols are numerical data, line is the analytical prediction given in Eq. (A3). Here $\Omega = 1, \gamma = 100$.

but with random hopping coupling:

$$H_{rnd} = -\Omega \sum_i (|i\rangle\langle i+1| + \text{H.c.}) + \sum_i E_i^0 |i\rangle\langle i|$$
$$- \gamma \sum_{i \neq j} \chi_{i,j} |i\rangle\langle j|. \qquad (B1)$$

Here the parameters are all the same of Eq. (1) apart from the fact that $\chi_{i,j} = \chi_{j,i}$ is a random number in the interval $(-1/2, +1/2)$. In this way the long-range coupling is random and it is easy to show that, in this case, there is no gap in the spectrum. This has important consequences on shielding. Indeed for random coupling the dynamics is never shielded from long-range hopping. To prove this we have computed the time needed for the fidelity, see Eq. (8), to decay to one
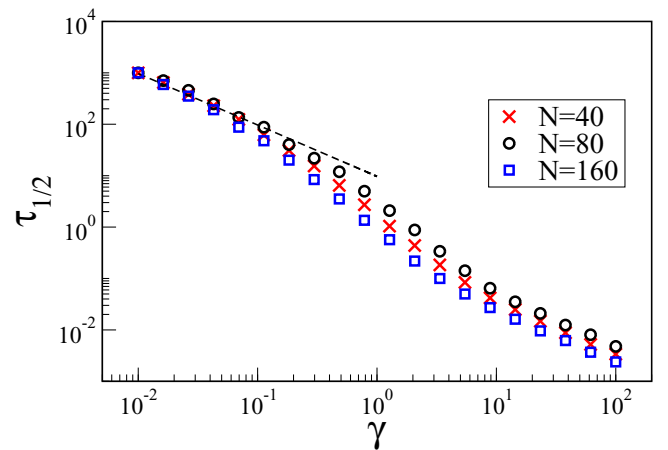

FIG. 14. Time needed to the fidelity to decay to one half, $\tau_{1/2}$ vs γ and different N values for the long-range random model in Eq. (B1). As initial state we choose a random superposition of all excited states. Dashed line stands for C/γ, where C is a fitting constant. Other data are $\Omega = 1, W = 100$ $\alpha = 0$. This figure should be compared with Fig. 7, which referred to homogeneous long-range hopping.
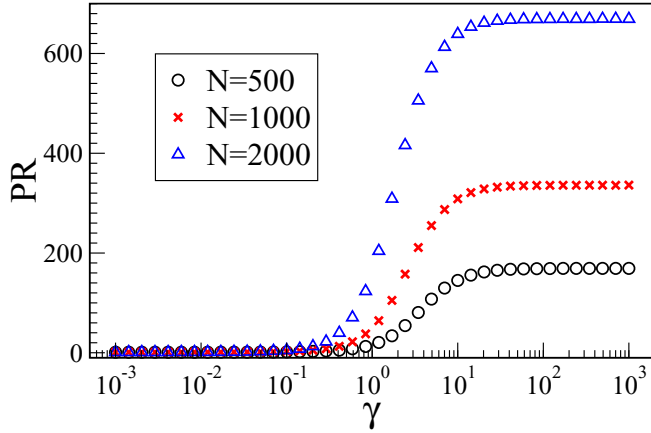
FIG. 15. Average (over all excited states) participation ratio vs γ, for different system size for the random long-range hopping described in Eq. (B1). Other parameters are $\Omega = 1, W = 100$. This figure should be compared with Fig. 11 (top).

half vs γ for different system sizes N. Results are shown in Fig. 14 where one can observe that $\tau_{1/2}$ always decays with γ, in contrast to the case of homogeneous long-range hopping where for $\gamma > \gamma_{\rm cr}$ $\tau_{1/2}$ becomes independent of γ. The absence of shielding in the random long-range model, also implies the absence of localization. This is shown in Fig. 15, where the PR is plotted as a function of γ. As one can see it increases up to a saturation point, which is proportional to the system size. This is at variance with the homogeneous long-range hopping, where the PR becomes independent of γ and N for $\gamma \gg \gamma_{\rm cr}$ as it is shown in Fig. 11 (top panel).

APPENDIX C: ENERGY GAP FOR POWER-LAW DECAYING LONG-RANGE HOPPING

Here we discuss the energy gap Δ_0 between the ground state and the first excited state in the one-dimensional periodic tight-binding model with long-range hopping and no on-site disorder, so that the Hamiltonian given in Eq. (11) can be written as:

$$H = -\Omega \sum_i (|i\rangle\langle i+1| + |i+1\rangle\langle i|) - \gamma \sum_{i \neq j} \frac{|i\rangle\langle j|}{r_{i,j}^\alpha} \quad \text{(C1)}$$

For any α, $[H_{NN}, V_{LR}] = 0$, and the common eigenstates are the same of that of Eq. (1) for $W = 0$. Indeed the eigenstates $|\psi_q\rangle$ can be computed exactly [17,18] and their components on the site basis $|k\rangle$, are independent of α and they can be written as:

$$\langle k | \psi_q \rangle = \frac{1}{\sqrt{N}} \exp\left(i \frac{2\pi kq}{N}\right) \quad \text{with} \quad q = 1, \ldots, N. \quad \text{(C2)}$$
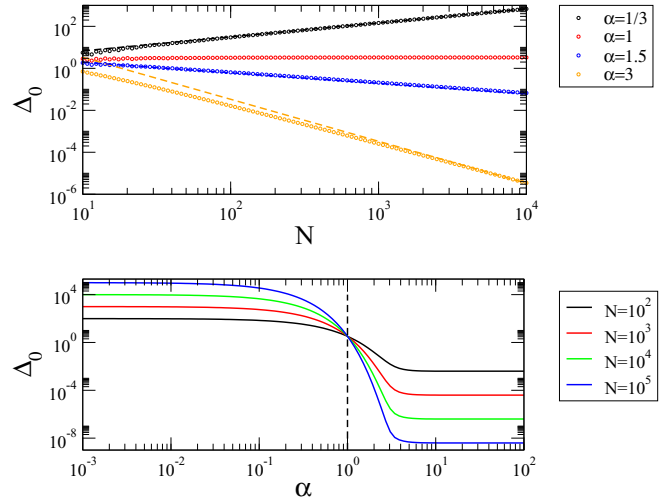

FIG. 16. Top: gap between the ground state and the first excited state Δ_0 vs the system size N for different values of α. Dashed lines are the asymptotic analytical predictions for Δ_0, see Eq. (12). Bottom: Δ_0 vs α for different N values. Data refer to the case of no disorder ($W = 0$) and $\Omega = \gamma = 1$, see Eq. (11).

For the eigenvalues of V_{LR}, we have [17,18]:

$$E_q^{LR} = \begin{cases} -2\gamma \sum_{n=1}^{N/2-1} \frac{\cos 2\pi qi/N}{n^\alpha} & N \quad \text{odd} \\ -\gamma \frac{(-1)^q}{(N/2)^\alpha} - 2\gamma \sum_{n=1}^{N/2-1} \frac{\cos 2\pi qi/N}{n^\alpha} & N \quad \text{even} \end{cases} \quad \text{(C3)}$$

Note that the ground state of V_{LR} for all α, corresponds to $q = N$ and it is the fully symmetric and extended state in the site basis, see Eq. (3).

For the case $\alpha = 0$, V_{LR} has only two eigenvalues different from zero: one nondegenerate, corresponding to the ground state, and one, which is $N - 1$ degenerate, corresponding to all the states orthogonal to it. For generic long range, the states orthogonal to the ground state are no longer all degenerate.

The eigenvalues of H_{NN} are

$$E_q^{NN} = -2\Omega \cos \frac{2\pi q}{N}. \quad \text{(C4)}$$

The common eigenvalues of $H_{NN} + V_{LR}$ are the sum of the eigenvalues of the two terms. For the ground state we have $E_N = -2\Omega + E_N^{LR}$. From these results we can compute the gap (energy difference between the ground state and the first excited state) Δ_0 for any α and the result is given in Eq. (12).

The analytical prediction about the energy gap is confirmed in Fig. 16. In Fig. 16 (top) the gap is plotted as a function of the system size for different values of α. We compare the asymptotic behavior given in Eq. (12) with numerical results, showing that Eq. (12) gives a very good estimate of the asymptotic behavior of the gap. In Fig. 16 (bottom) the gap is plotted as a function of α for different system sizes. As one can see for long-range hopping $\alpha < 1$, the gap increases with the system size, it is constant for the critical case $\alpha = 1$, and it decreases with N for $\alpha > 1$.

[1] J. Grad, G. Hernandez, and S. Mukamel, Phys. Rev. A **37**, 3835 (1988); F. C. Spano, J. R. Kuklinski, and S. Mukamel, J. Chem. Phys. **94**, 7534 (1991); R. Monshouwer, M. Abrahamsson, F. van Mourik, and R. van Grondelle, J. Phys. Chem. B **101**, 7241 (1997); M. Mohseni, P. Rebentrost, S. Lloyd, and A. Aspuru-Guzik, J. Chem. Phys. **129**, 174106 (2008); G. L. Celardo *et al.*, J. Phys. Chem. C **116**, 22105 (2012); D. Ferrari, G. L. Celardo, G. P. Berman, R. T. Sayre, and F. Borgonovi, *ibid.* **118**, 20 (2014).

[2] J. Schachenmayer, C. Genes, E. Tignone, and Guido Pupillo, Phys. Rev. Lett. **114**, 196403 (2015); J. Feist and F. J. Garcia-Vidal, *ibid.* **114**, 196402 (2015).

[3] C. W. J. Beenakker, Rev. Mod. Phys. **69**, 731 (1997); S. Sorathia, F. M. Izrailev, V. G. Zelevinsky, and G. L. Celardo, Phys. Rev. E **86**, 011142 (2012); A. Ziletti, F. Borgonovi, G. L. Celardo, F. M. Izrailev, L. Kaplan, and V. G. Zelevinsky, Phys. Rev. B **85**, 052201 (2012).

[4] P. Jurcevic *et al.*, Nature (London) **511**, 202 (2014); P. Hauke and L. Tagliacozzo, Phys. Rev. Lett. **111**, 207202 (2013); M. Cheneau *et al.*, Nature (London) **481**, 484 (2012); P. Richerme *et al.*, *ibid.* **511**, 198 (2014).

[5] E. Akkermans, A. Gero, and R. Kaiser, Phys. Rev. Lett. **101**, 103602 (2008); R. Kaiser, J. Mod. Opt. **56**, 2082 (2009); T. Bienaime, N. Piovella, and R. Kaiser, Phys. Rev. Lett. **108**, 123602 (2012); E. Akkermans and A. Gero, Europhys. Lett. **101**, 54003 (2013).

[6] F. Borgonovi, G. L. Celardo, M. Maianti, and E. Pedersoli, J. Stat. Phys. **116**, 1435 (2004); D. Mukamel, S. Ruffo, and N. Schreiber, Phys. Rev. Lett. **95**, 240604 (2005).

[7] R. Bachelard, C. Chandre, D. Fanelli, X. Leoncini, and S. Ruffo, Phys. Rev. Lett. **101**, 260603 (2008)

[8] D. Métivier, R. Bachelard, and M. Kastner, Phys. Rev. Lett. **112**, 210601 (2014).

[9] D.-M. Storch, M. van den Worm, and M. Kastner, New J. Phys. **17**, 063021 (2015).

[10] L. F. Santos, F. Borgonovi, and G. L. Celardo, Phys. Rev. Lett. **116**, 250402 (2016).

[11] L. S. Levitov, Europhys. Lett. **9**, 83 (1989); Phys. Rev. Lett. **64**, 547 (1990); F. Evers and A. D. Mirlin, Rev. Mod. Phys. **80**, 1355 (2008).

[12] H. N. Nazareno and P. E. de Brito, Phys. Rev. B **60**, 4629 (1999).

[13] A. Ossipov, J. Phys. A **46**, 105001 (2013).

[14] G. L. Celardo, A. Biella, L. Kaplan, and F. Borgonovi, Fortschr. Phys. **61**, 250 (2013); A. Biella, F. Borgonovi, R. Kaiser, and G. L. Celardo, Europhys. Lett. **103**, 57009 (2013).

[15] G. G. Giusteri, F. Mattiotti, and G. L. Celardo, Phys. Rev. B **91**, 094301 (2015); G. L. Celardo, Giulio G. Giusteri, and F. Borgonovi, *ibid.* **90**, 075113 (2014).

[16] T. Dauxois, S. Ruffo, E. Arimondo, and M. Wilkens, *Lecture Notes in Physics*, Vol. 602 (Springer, Berlin, 2002).

[17] F. A. B. F. de Moura, A. V. Malyshev, M. L. Lyra, V. A. Malyshev, and F. Dominguez-Adame, Phys. Rev. B **71**, 174203 (2005).

[18] J. Barré, Physica A **305**, 172 (2002).

[19] R. Modak, S. Mukerjee, E. A. Yuzbashyan, and B. S. Shastry, New J. Phys. **18**, 033010 (2016); J. von Delft, Annalen der Physik (Leipzig) **10**(3), 219 (2001); H. K. Owusu, K. Wagh, and E. A. Yuzbashyan, J. Phys. A **42**, 035206 (2009).

[20] L. del Re, M. Fabrizio and E. Tosatti, Phys. Rev. B **93** 125131 (2016).

[21] P. W. Anderson, Phys. Rev. **109**, 1492 (1958).

[22] M. Hastings and T. Koma, Commun. Math. Phys. **265**, 781 (2006).

[23] J. Schachenmayer, B. P. Lanyon, C. F. Roos, and A. J. Daley, Phys. Rev. X **3**, 031015 (2013).

[24] J. Eisert, M. van den Worm, S. R. Manmana, and M. Kastner, Phys. Rev. Lett. **111**, 260401 (2013).

[25] Z.-X. Gong, M. Foss-Feig, S. Michalakis, and A. V. Gorshkov, Phys. Rev. Lett. **113**, 030602 (2014).

[26] L. Mazza, D. Rossini, M. Endres, and R. Fazio, Phys. Rev. B **90**, 020301 (2014).

[27] M. Foss-Feig, Z.-X. Gong, C. W. Clark, and A. V. Gorshkov, Phys. Rev. Lett. **114**, 157201 (2015).

[28] E. H. Lieb and D. W. Robinson, Commun. Math. Phys. **28**, 251 (1972).

[29] A. Rodriguez, V. A. Malyshev, G. Sierra, M. A. Martin-Delgado, J. Rodriguez-Laguna, and F. Dominguez-Adame, Phys. Rev. Lett. **90**, 027404 (2003); A. Rodriguez, V. A. Malyshev and F. Dominguez-Adame, J. Phys. A **33**, L161 (2000).

[30] N. Kroó, P. Rácz, and S. Varró, Europhys. Lett. **105**, 67003 (2014).